

Location and character of volatile general anesthetics binding sites in the vallinoid receptor

Christian Jorgensen^a and Carmen Domene^{b,c,*}

^aDepartment of Chemistry, Britannia House, 7 Trinity Street, King's College London, London SE1 1DB, UK, ^bDepartment of Chemistry, University of Bath, 1 South Building, Claverton Down, Bath BA2 7AY, UK, ^cChemistry Research Laboratory, Mansfield Road, University of Oxford, Oxford OX1 3TA, UK

*Corresponding author: C.Domene@bath.ac.uk Tel: +44 - (0)1225-386172

Abstract

It has been proposed that general anesthesia results from direct multisite interactions with multiple and diverse ion channels in the brain. An understanding of the mechanisms by which general anesthetics modulate ion channels is essential to clarify their underlying behavior and their role in reversible immobilization and amnesia. Volatile general anesthetics are drugs that primarily induce insensitivity to pain, however, they sensitize and activate TRPV1, which is known to mediate the response of the nervous system to certain harmful stimuli and plays a crucial role in the pain pathway. Currently, the mechanism of action of general volatile anesthetics and the precise molecular sites of interaction are unknown. Here, using $\sim 2.5 \mu\text{s}$ of classical MD simulations in combination with free energy and enhanced sampling techniques, we explore these enigmas. Binding sites are identified and the strength of their association is further characterized using alchemical free-energy calculations. Anesthetic binding/unbinding proceeds primarily through a membrane-embedded pathway, and subsequently, a complex scenario is established involving multiple binding sites featuring single or multiple occupancy states. One of the five binding sites reported was previously identified experimentally, and another one is identical to that of capsaicin, a TRPV1 agonist. However, isoflurane and chloroform binding free-energies render modest to no association compared to capsaicin, suggesting a different activation mechanism. Our simulations suggest that these drugs do not induce new conformational states but rather only bind to pre-existing ones and could exert their effects simply by shifting the equilibrium in favour of those conformations that contain anaesthetic-binding sites and in competition with TRPV1 agonists.

Introduction

It has been proposed that general anesthesia results from direct multisite interactions with multiple and diverse ion channels in the brain.¹ Experimental findings of volatile general anesthetics binding to ion channels comes from structural work, where crystal structures of ion channels were obtained in complex with volatile general anesthetics,²⁻⁵ as well as mutagenesis⁶ and photolabelling⁷ studies. In particular, evidence of a modulation mechanism for anesthetics on both the nAChR (nicotinic acetylcholine) and GABAA receptors involving multiple binding sites has been described experimentally.⁸⁻¹⁰ In parallel, computational studies have yielded insights into volatile general anesthetics binding in membrane proteins,¹¹⁻¹⁴ including simulations using a supersaturated isoflurane concentration suggesting that the modulation of nAChR and GLIC ion channels, occurs by binding to multiple sites.¹¹ In sodium channels, microsecond simulations of NavAb revealed a similar multiple-binding site model for volatile general anesthetics benzocaine and phenytoin, and yielded two drug-access pathways into the pore, a lipophilic access pathway through lateral fenestrations, and an aqueous pathway through the intracellular activation gate.¹² At present, there is growing evidence that most general and local anesthetics as well as some analgesics also activate or sensitize nociceptors via TRPA1 or TRPV1 ion channels.¹⁵⁻¹⁶ Activation and sensitization of TRPV1 induced by local anesthetics is thought to involve a domain that is similar but not identical to the vanilloid-binding domain, the area of the protein that interacts with its agonist.

Volatile general anesthetics span a group of chemicals that are able to reversibly inhibit the central nervous system activity, rendering patients unresponsive to stimuli in contrast to local anesthetics. Little is known about the molecular targets of inhaled anesthetics to relate their effect to pharmacology. However, their binding sites are known to be hydrophobic with some polar character and with sufficiently general features to be widespread.¹⁷ Volatile general anesthetics including isoflurane (1,1,1-trifluoro-2-chloro-2-(difluoromethoxy)-ethane), chloroform, propofol, and halothane are reported to bind directly to ion channels.^{3-4, 18-19} In contrast to their inhibitory effects on the central nervous system, several volatile general anesthetics are known to activate or sensitize the signaling of peripheral nociceptive (pain-sensing) neurons²⁰ which gives origin to their pungency or the condition of having a strong and sharp smell or taste that can be unpleasant.

The transient receptor potential (TRP) ion channels constitute a large and diverse family of non-selective cation channels, found in yeast and widespread in the animal kingdom.²¹ These channels are expressed in excitable and non-excitable cell tissue, playing a critical role in sensory physiology by acting at the cell level, including synaptic activity or hormone secretion, and at organism levels (tactile, hearing, taste, olfaction, vision and thermal sensation).²¹⁻²² TRP channels display multifunctional and polymodal behavior in their regulation and interactions. In particular, the vanilloid-1 channel (TRPV1), arguably the best-characterized member of the vertebrate TRP family, is activated by a diverse array of physical and chemical stimuli such as noxious heat, inflammatory agents, such as extracellular protons

and lipids, or capsaicin, the active compound of chili peppers that elicits burning pain.²³ Upon capsaicin stimulation, the channel undergoes pore dilation, in which its selectivity for large cations over sodium ions is increased. While a single capsaicin-bound subunit was sufficient to achieve maximal open-channel lifetime, all four proton-binding sites were required. Therefore, the pain receptor TRPV1 was reported to display agonist-dependent activation stoichiometry.²⁴

Chloroform became the most popular volatile general anesthetic of the 19th century, before being abandoned because of its low therapeutic index,¹⁹ but has recently regained interest as having been reported to activate the TRPV1 ion channel at millimolar concentrations using a similar mechanism as isoflurane. In particular, experimental data has suggested that TRPV1 is directly activated by chloroform, and none of the other heat-activated channels (TRPV2, TRPV3 or TRPV4) are activated by chloroform at clinical concentrations that are reported to elicit a robust activation of TRPV1.¹⁹

Chloroform at a concentration of ~6.3 mM had solely an additive effect on channel activation when administered in the presence of capsaicin concentrations of ≤ 5 nM, while at concentrations ≥ 10 nM capsaicin yielded indistinguishable activation in the presence or absence of chloroform.¹⁹ It has been postulated that residue E600 is required for proton and volatile general anesthetics activation, and Y653 is required for heat and volatile general anesthetics activation of TRPV1,¹⁹ and that these two residues, E600 and Y653, might facilitate channel activation.²⁵ Recent structural and biophysical studies have resolved the atomic structures of some of the members of the TRP family primarily by cryo-electron microscopy.^{23, 25} These structural models provide an excellent starting point for the mechanistic study of anesthetic interactions and binding at the molecular level.

From the cryo-EM structure it is known that the TRPV1 channel architecture consists of a tetrameric assembly of four monomeric subunits, analogous to those of voltage-gated sodium and potassium channels. Each subunit consists of six trans-membrane α -helices (S1–S6) and an S5-P-S6 pore loop–helix (Figure 1.A). Previously, computational studies reported cation binding sites in the pore domain of TRPV1,^{26,27} in particular confirming the capsaicin binding poses (Figure 1.A).²⁸ Here, we attempt to explore the nature of the activation pathways evoked by two volatile general anesthetics in TRPV1, chloroform and isoflurane (Figure 1.B), compare them with capsaicin, and narrow down putative interaction sites hinted in experimental studies. The system setup is illustrated in Figure 1.C.

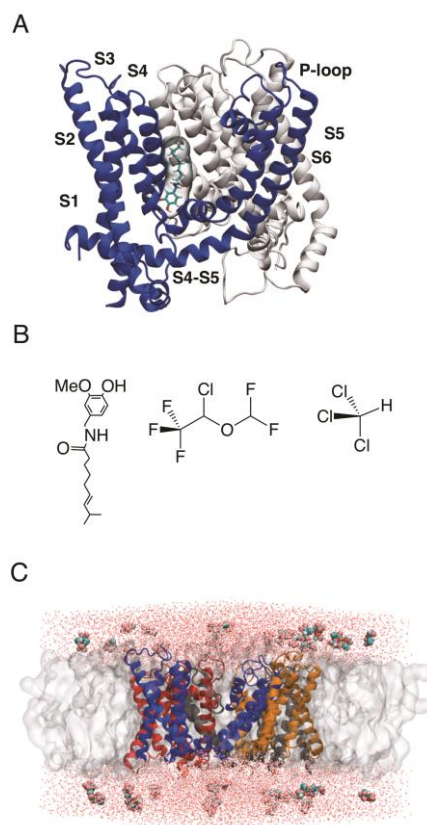


Figure 1. (A) Two TRPV1 subunits shown in blue and white respectively and the capsaicin binding site reported in structural studies.²⁸ Capsaicin is shown in licorice representation, and the structural elements of one of the monomers are labelled (helices S1 to S6 and P-loop connecting helices S5 and S6). (B) Chemical structure of capsaicin, isoflurane and chloroform respectively. (C) Simulation setup for the TRPV1 transmembrane region in purple where only two out of the four monomers are shown for clarity, and with an initial random distribution of volatile anesthetics in solution in the bulk.

Materials and Methods

System set-up

The atomic model of the apo transmembrane region of the vanilloid receptor 1 (TRPV1) was retrieved from the protein data bank, PDB ID 3J5Q,²⁵ at resolution 3.4 Å (residues V430 to V686). The set-up was done with CHARMM-GUI (<http://www.charmm-gui.org>).²⁹ The N-terminus was acetylated and the C-terminus was methylated. The CHARMM36 force field with CMAP corrections was used for the protein³⁰⁻³¹ and lipids³² together with the TIP3P model for water molecules.³³ CHARMM force field parameters for isoflurane³⁴ and chloroform³⁵ were used. Default ionization states were used for the protein on the basis of PropKa calculations.³⁶ The protein was embedded in a pre-equilibrated lipid bilayer of 240 POPC (1-palmitoyl, 2-oleoyl-sn-glycero-3-phosphocholine) lipids using the replacement method of CHARMM-GUI, with 120 lipids in the upper-layer, and 120 lipids in the lower layer, with the axis aligned to the bilayer normal. The system was embedded in a rectangular water box of dimensions (110, 110, 85) Å³. A 150 mM KCl solution was added to neutralize the system. The full TRPV1 pore system (residues V430-V686) comprised ~90,000 atoms, while the pore model (E570-V686) comprised ~50,000 atoms. The total concentration of isoflurane and chloroform added independently was 8 mM to facilitate sufficient statistics.

Equilibration was done using NAMD version 2.9³⁷ starting with 5,000 steps of steepest-descent minimization, 75 ps of dynamics in the NVT ensemble with restraints on the backbone with a time-step of 1 fs, followed by 300 ps of dynamics in the NVT ensemble with restraints on the backbone with a time-step of 2 fs. Finally, the system was evolved 1.0 ns in the NPT ensemble. The output of the MD equilibration was used as the starting point for two subsequent sets of MD production runs with (i) 40 isoflurane or (ii) 40 chloroform molecules (Figure 1.C). Production runs of the flooding simulations were performed in the NPT ensemble. A summary of the simulations performed is reported in the Supplementary Material Table S1. The particle mesh Ewald (PME) algorithm was used for the evaluation of electrostatics interactions beyond 12 Å, with a PME grid spacing of 1 Å, and NAMD defaults for spline and κ values.³⁸ A cut-off at 12 Å was applied to non-bonded forces. Both electrostatics and Van der Waals forces were smoothly switched off between the cut-off distance of 12 Å and the switching distance of 10 Å, using the default NAMD switching function. A Verlet neighbor list with pairlist distance of 16 Å was used to only evaluate non-bonded neighboring forces within the pairlist distance³⁹. The lengths of covalent bonds involving hydrogen atoms were constrained by the SETTLE algorithm⁴⁰ in order to be able to use a 2-fs time-step. The multi time step algorithm Verlet-I/r-RESPA^{39, 41} was used to integrate the equations of motion. Non-bonded short-range forces were computed for each time step, while long-range electrostatic forces were updated every 2 time steps. The pressure was kept at 1.013 atm by the Nosé-Hoover Langevin piston⁴²⁻⁴⁴ with a damping time constant of 25 fs and a period of 50 fs. The temperature was maintained at 303.15 K by coupling the system to a Langevin thermostat, with a damping coefficient of 1 ps⁻¹.

Free energy of insertion of anesthetics in the membrane

In order to estimate the partitioning free energies of isoflurane and chloroform in the membrane, estimates of the free energy of insertion in the POPC lipid bilayer were calculated using metadynamics⁴⁵ with a funnel-restrained potential,⁴⁶ enabling the exploration of both the unbound bulk and lipid-partitioned states. A schematic representation of the restraint setup is presented in Figure S1.A. An equilibrated bilayer of 100 POPC molecules with just one anesthetic molecule was set up, with a 0.15 mM background KCl. A funnel-restrained well-tempered metadynamics⁴⁵ calculation using the collective variable ξ_1 as the distance along the Z-axis, where 1 = 0 Å constitutes the membrane centre, and 35 Å the bulk. In addition, ξ_2 is the radial distance of the drug in the funnel, as measured from the Z-axis, and corresponding to the transversal funnel degree of freedom. This simulation was performed using Plumed 1.3⁴⁷ with NAMD 2.9, with a Gaussian deposited every 1 ps of width of 0.2 Å and initial height 0.12 kcal/mol using a bias factor of 12. The funnel-restrained potential is a combination of a cone restraint, which includes the external side of the membrane, and a cylindrical part, which is directed toward the solvent.⁴⁶ The alpha angle, α , denoting the funnel angle from the normal axis, was set to 0.55 rad (31.5°), Z_{cc} the funnel height to 35 Å, placed at the center of the membrane. A geometric correction term (Equation 1), is added to the free-energy, ΔG , to give the free-

energy of translocation from the bulk into the membrane, ΔG° , by computing the geometric contribution from the bulk cylinder of $R_{\text{cyl}} = 1 \text{ \AA}$, scaled by the standard concentration $C^\circ = 1 \text{ mol dm}^{-3} = 1/1661 \text{ particles \AA}^{-3}$, which yields a correction term of $-3.7 \text{ kcal mol}^{-1}$. The value of the collective variable is monitored in Supplementary Material Figure S1.C. The ΔG for isoflurane obtained was $-7.0 \text{ kcal mol}^{-1}$ (Supplementary Material Figure S1.B), and $-6.3 \text{ kcal mol}^{-1}$ for chloroform (Supplementary Material Figure S1.B). The corrected free-energies (ΔG°) were -3.3 and $-2.6 \text{ kcal mol}^{-1}$ for isoflurane and chloroform, respectively.

$$\Delta G^\circ = \Delta G - \frac{1}{b} \ln(pR_{\text{cyl}}^2 C^\circ) \quad \text{Equation 1}$$

An error analysis was performed by obtaining the average potential of mean force of the plateau region (last 100 ns of simulation). Upon geometric averaging, a standard deviation of 0.6 and 0.8 kcal mol^{-1} for isoflurane and chloroform were obtained.

Standard free energy of binding of anesthetics to TRPV1

The free energy of binding, ΔG_{bind} , of each anesthetic to TRPV1 was calculated and compared to the binding energy of the TRPV1 agonist capsaicin.²⁸ The value of the free energy of binding of capsaicin to TRPV1 was reported²⁸ to be $-10.6 \pm 1.7 \text{ kcal mol}^{-1}$ obtained using the method by Gumbart et al.⁴⁸ A schematic representation of the cycle is presented in Figure S2.A, and shown exemplified by isoflurane in Figure S2.B. This method relies upon alchemical free-energy perturbation transformations, combined with geometrical restraints on the anesthetics to avoid the wandering ligand problem at the end of the decoupling or beginning of coupling simulations.⁴⁹⁻⁵⁰ Reversible coupling of the anesthetic to its environment, either bulk aqueous solution (unbound state) or the TRPV1 pocket (bound state), was performed bi-directionally using the free energy perturbation (FEP) method. The order parameter λ was evenly divided into 16 windows of width equal to 0.05 in the range 0.1 to 0.9, plus 40 windows of width equal to 0.005, in the range 0 to 0.1 and 0.9 to 1.0. Each window consisted of 200,000 data collection steps (0.4 ns), preceded by 50,000 equilibration steps (0.1 ns). The total simulation time was 28 ns per coupling/decoupling cycle, totaling 54 ns for the bound state, and 54 ns for the unbound state. The total simulation time employed for the alchemical FEP calculations was 216 ns.

The convergence of the alchemical calculations was evaluated by analyzing the overlap of the ΔU distributions for the forward (ΔU_0) and backward (ΔU_1) calculations, per window (Figure S3). The statistical data was combined by means of the Bennett acceptance ratio (BAR)⁵¹ which provides a maximum-likelihood estimator of the free-energy change.⁵² The ParseFEP tool⁵³ implemented in VMD⁵⁴ was used to analyze the results. To prevent the wandering ligand problem, the conformation of anesthetic was restrained during the free-energy calculations, and each calculation was based on the central cluster node from the MD binding site II'' (capsaicin binding site) occupied in one of the four TRPV1 subunits. Geometrical restraints were defined based on three invariant protein reference sites

(P1, P2, P3). These sites were defined as the center of mass (COM) of heavy atoms of residues A566, F582 and L664. In addition, three reference sites in the anesthetic molecules (L1, L2, L3) were defined. These sites correspond to the center of mass of selected pairs of atoms in isoflurane or chloroform. In total, six sites were used to define the harmonic restraints u_r (distance P1–L1), u_θ (angle P2–P1–L1), and u_ϕ (dihedral P3–P2–P1–L1) used to fix the position of the anesthetic molecule in the protein pocket. U_θ (angle P1–L1–L2), u_ϕ (dihedral P1–L1–L2–L3), and u_ψ (dihedral P2–P1–L1–L2) were used to fix the anesthetic orientation. Finally, a harmonic RMSD restraint on the conformation of the anesthetic molecule (u_c) ensured the pose was fully fixed. To estimate the contribution to the free energy of binding as a result of the restraints, thermodynamic integration (TI) simulations were performed coupling the force constant of each harmonic potential to the order parameter λ in a 12-point grid. The gradient of the potential energy with respect to the collective variable was calculated from MD simulations at each value of λ . Each simulation consisted of 200,000 data collection steps (0.4 ns), after 50,000 steps (0.1 ns) of equilibration. Scaling of the force constants was also performed bi-directionally, and the free energy contribution of the restraints was retrieved averaging both contributions. The error was estimated as the maximum hysteresis between forward and backward calculations.

Docking procedure

Docking of anesthetics was performed using Autodock (v4.2) on the full TRPV1 pore (V430-V686).⁵⁵ Two dockings were performed, one based on the holo-TRPV1 trajectory (PDB id 3J5Q; Resolution 3.8) and the second based on an apo-TRPV1 trajectory (PDB id 3J5P; Resolution 3.4 Å). At the start, 500 snapshots were extracted at equal intervals between 50 to 150 ns, discarding 50 ns for equilibration. Then, 300 snapshots were extracted, discarding 50 ns of equilibration. For both apo and holo trajectories, a global search was carried out with a large box centered on the protein and employing 140 x 140 x 110 grid points, with default grid spacing of 0.375 Å. For each docking snapshot, 10 solutions were requested. Altogether, 5,000 and 3,000 docking poses were generated, respectively, which were later clustered according to the RMSD of the ligand using a RMSD < 2.5 Å criteria per cluster.

Results

Partition of anesthetics in the lipid bilayer

An interaction between inhalational anaesthetics and proteins was first suggested by Claude Bernard in 1875,⁵⁶ and subsequently by Moore and Roaf in 1904 and 1905⁵⁷⁻⁵⁸ (see reference [17] for a detailed historical account). In contrast, Meyer, Overton, and others, proposed that the lipid membrane of the cell was generally to be the primary site of action of anesthetics.⁵⁹⁻⁶⁰ Recent work continues to suggest a membrane-mediated mechanism whereby chemical compounds may modify the properties of the cell membrane, which in turn, would alter the properties of the proteins embedded in the cell membrane. Alternatively, anaesthetics would need to cross the water-membrane interphase until they reach specific sites in the protein and as a result of these interactions the protein gating and permeation properties will

be altered. Currently, the favoured hypothesis proposes that general anesthesia results from direct multisite interactions with multiple and diverse ion channels in the brain as gradually, a number of important molecular targets have emerged. In this respect, how volatile general anesthetics act at the molecular level is becoming clearer.

In this respect, two 0.5- μ s MD flooding simulations of either isoflurane or chloroform partitioning into a fully solvated TRPV1 transmembrane domain inserted in a POPC bilayer were performed. Overall, the protein is stable during the simulation time even in the presence of a high clinical concentration of anesthetic; analysis of the protein all-atom backbone root-mean-square deviation was 2.2 ± 0.2 Å and 2.7 ± 0.3 Å, respectively (Supplementary Material Figure S4 and Table S1). These values are within the resolution of the model structure employed indicating that equilibration was achieved. Chloroform and isoflurane can affect the TRPV1 ion channel by partitioning into the plasma membrane, a process facilitated by hydrophobic interactions with the inner-membrane core, and then modify the properties of the bilayer, or alternatively, they can reach the transmembrane region of the protein and compete with capsaicin and other activators. In this context, while both chloroform and isoflurane have moderate lipophilicity⁶¹ (logP 2.0 and 2.1, respectively), chloroform possesses a dipole moment (9.5 Å³) and has been found to display a slight preference for the membrane core.⁶² Isoflurane, in contrast, is a non-hydrophobic anesthetic,^{34, 63} which readily partitions into the lipophilic phase, but shows a preference for the interfacial regions, with some studies suggesting that it does not readily accumulate in the hydrophobic membrane core.^{11, 64} The behavior of other TRPV1 agonists, such as camphor (logP 2.2) is similar to isoflurane, showing preference for the interface, meaning its therapeutic dose is higher than for other agonists.⁶⁵ Strikingly, despite the relatively high concentration required for activation and potentiation of TRPV1, the effects of camphor were found to be rapidly and readily reversible and a mechanical rather than a biochemical link to the pore gating machinery was proposed.⁶⁵

The cost of moving isoflurane from the bulk solution to the polar head group interface of a POPC bilayer had previously been reported to be ≈ 4 kcal mol⁻¹ using umbrella sampling simulations.⁶⁶ Similarly, here, an 0.8- μ s well-tempered metadynamics simulation with funnel restraints rendered a free-energy for translocation between the bulk solution and the membrane center of -3.4 ± 0.6 and -2.5 ± 0.8 kcal mol⁻¹ for isoflurane and chloroform, respectively. In the current study, both anesthetics partition readily to the membrane phase (Figure 2.A) reaching 95% and 90% for isoflurane and chloroform respectively after 200 ns of simulation time (Figure 2.B), and no distortion of the lipid membrane was observed upon partitioning, as had already been reported in earlier simulations of isoflurane and similar VGAs.⁶⁶ On the whole, the lipophilic entry route is the primary access mode for these anesthetics to their protein binding sites, as illustrated for two diffusion paths of membrane-partitioned isoflurane and chloroform as monitored by the ligand RMSD over trajectory time (Figure 2.C) and depicted as iso-contour trajectory probability in Figure 2.D. Only 5% isoflurane molecules and

10% of chloroform do not reach their binding via membrane partitioning. The secondary pathway (Figure 2.A) is a direct entry into the protein from the bulk (Figure 2.A).

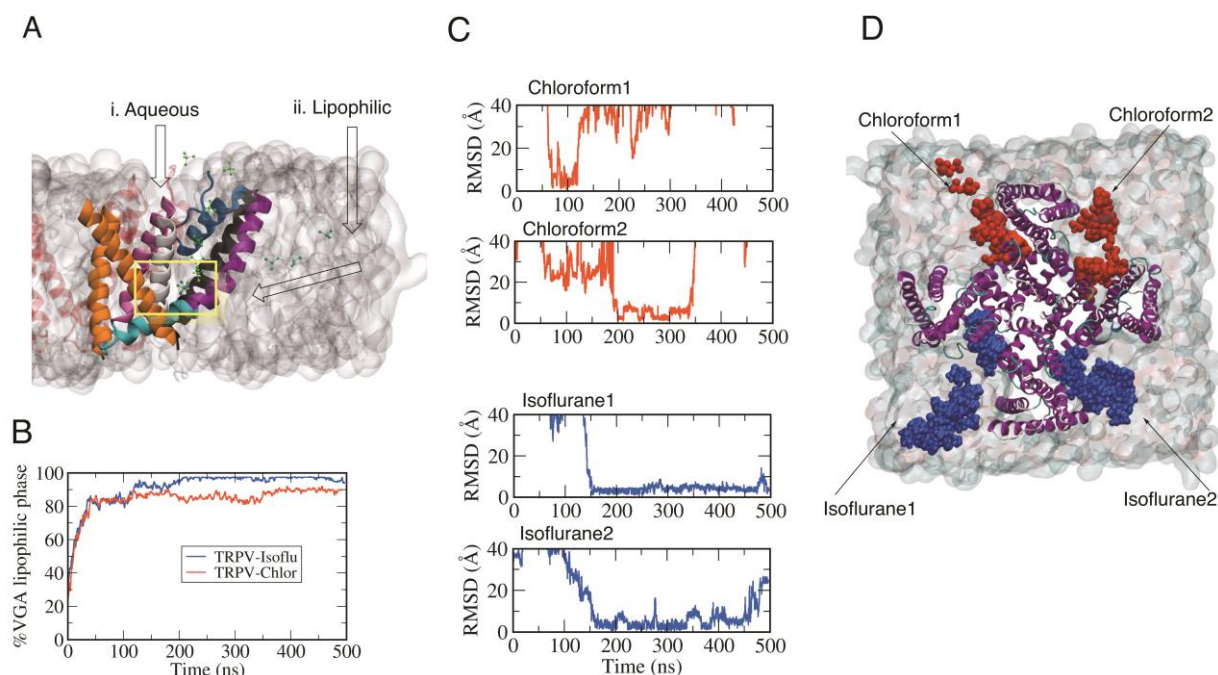


Figure 2. (A) Schematic comparison of the lipophilic and aqueous entry routes. The lipid membrane is depicted in grey color and one out of the four monomers composing the transmembrane domain of the ion channels is depicted in ribbon representation with each transmembrane helix colored differently. (B) Percentage (%) of anesthetics partitioning into the membrane for isoflurane (color code blue; plateau 95%) and chloroform (color code red; plateau 90%) as a function of simulation time. (C) Evolution of the ligand RMSD with respect to its bound pose for two isoflurane (blue) and two chloroform (red) molecules. Each molecule is labeled 1 or 2. (D) Illustration of the entry pathway through the membrane observed for each of the two chloroform and isoflurane molecules considered, looking from above the lipid membrane and indicated by arrows. Please note that this illustration was produced from a superposition of frames from two independent simulations.

Upon reaching the inner transmembrane region, five binding sites were identified using iso-contour projections (Figure 3.A and B): (a) a pore site, site I (Figure 3.C), (b) the same site capsaicin occupies, site II' (Figure 3.D), (c) two side-pocket sites and III, and finally (e) site IV, within the outer helices (Figure 3.E). The protein-anesthetic contacts identified are described in detailed in Table S2 and are graphically summarized in for three key sites (Figure 3.C,D,E). The binding sites were validated by projections of the chloroform free-energy surface (Figure 4.A) compared to the iso-contour probabilities (Figure 4.B) and the same for isoflurane (Figure 4.C to 4.D). The stability of the binding poses is characterized by the ligand root mean square deviation relative to the binding pose in each site, as illustrated for representative anesthetic trajectories in Figure 2.C and in full in Supplementary Material Figure S5. The difference in interactions between the protein and both anesthetics suggests chloroform and isoflurane bind differently to TRPV1. The difference can be ascribed to the smaller size of chloroform which allows for sampling regions that are not accessible to isoflurane, resulting in two additional sites accessible to chloroform, site II and III, which are variants of the side-pocket site II' of capsaicin.

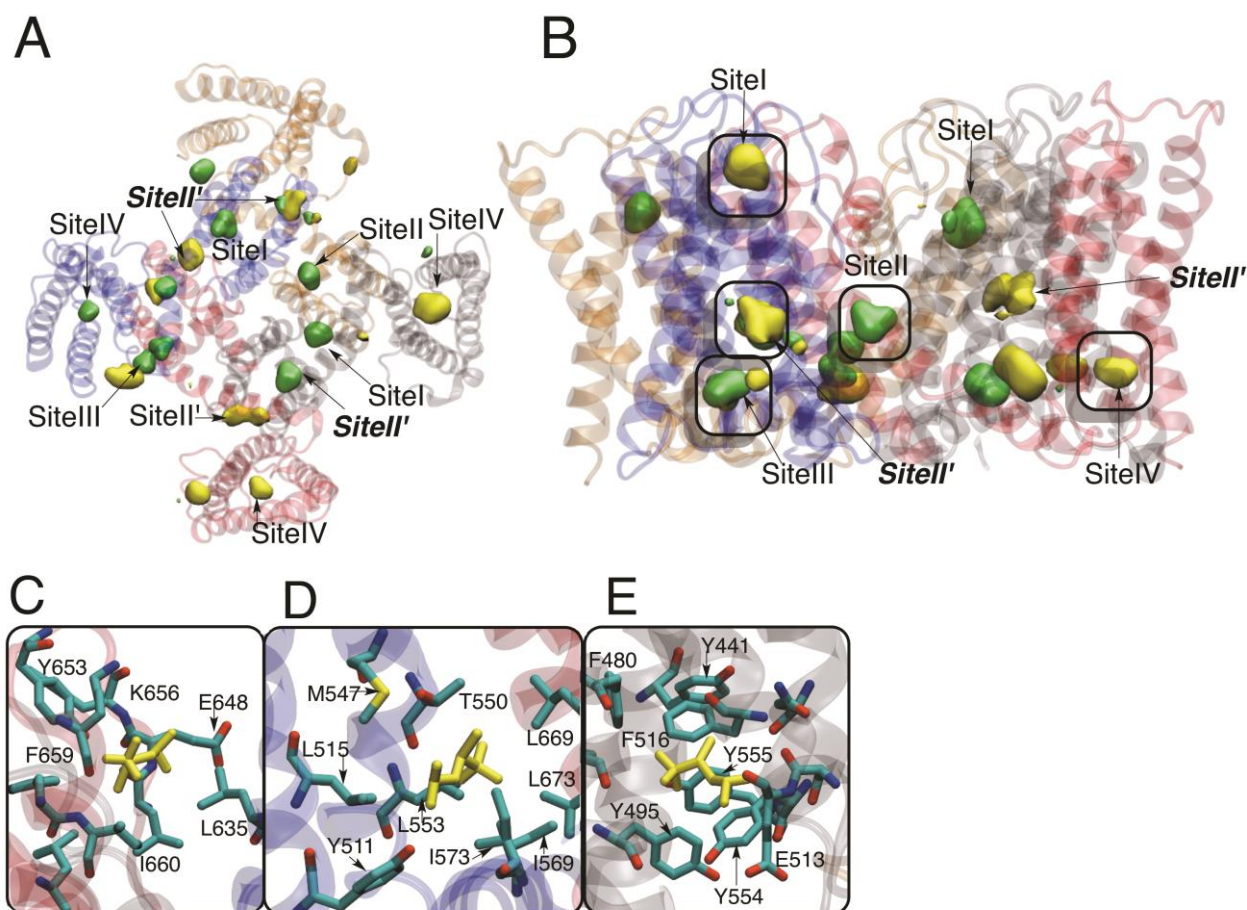


Figure 3. Population density analysis for isoflurane (yellow) and chloroform (green) for the MD simulations using the full pore. (A) View of the system from the intracellular side, and (B) from XZ plane of the membrane. Based on 500 ns of trajectory, an iso-0.2 contour criterion was employed for delimiting population, which shows iso-20% surfaces. (C, D, E) protein-anesthetic contacts denoted in for key individual sites, for (C) site I, (D) site II' and (E) site IV.

The iso-contour surfaces were used to generate a full probability distribution $Z(\xi)$ of anesthetics during the MD simulation, which, when Boltzmann-weighted, give the free-energy surface (FES) projected onto the xy ($\xi(x,y)$) and xz ($\xi(x,z)$) planes:

$$F(\xi) = -kT \log (Z(\xi)/Z_0) \quad \text{Equation 2}$$

This final distribution (Figure 4.A and 4.C for chloroform and isoflurane respectively) is comparable to the iso-probability contour surfaces of chloroform (Figure 4.B) and isoflurane (Figure 4.D). Five binding sites constitute minima on the FES, where the most long-lived binding sites I, II' and IV are separated by up to 3 kcal mol⁻¹ from the bulk, which readily agrees with our estimate of binding free energy for chloroform and the free-energy gain of membrane-partitioning. This projection also reveals the membrane-partitioned pathway to constitute a Minimum Free-Energy Path (MFEP), in agreement with the up to 4 kcal mol⁻¹ binding affinity of local anesthetic binding benzocaine in flooding simulations of Nav channels when compared to the bulk configuration.⁶⁷

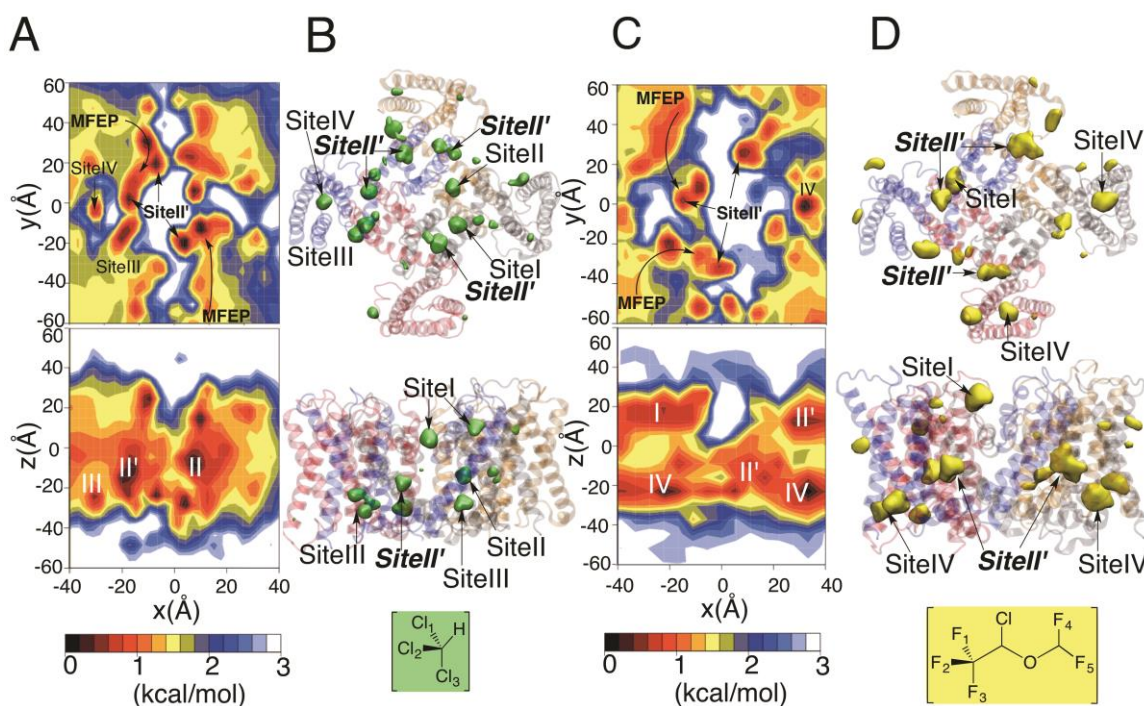


Figure 4. Classification of anesthetic binding sites according to their free-energy maps. XY and XZ surface projections of the free energy surfaces (FES) from the intracellular side for (A) chloroform and (C) isoflurane. The construction of the maps is detailed in the Methods section. Binding sites are labelled from I to IV. The minimum free energy pathway from the bulk solution to the binding site is indicated with black arrows. Based on two 500-ns of trajectory, an iso-0.2 contour criterion was employed for delimiting populations which shows iso-20% density surfaces illustrated for (B) chloroform (green) and (D) isoflurane (yellow) using a top or side view of the channel with respect to the membrane normal.

From the detailed residue analysis in Figure 3.C, the anesthetic binding site I is flanked by two TRPV1 monomers and located at the pore (P)-loop region. Isoflurane and chloroform share two contacts when bound in Site I of TRPV1, L635 and I660 (Supplementary Material Table S2). In addition, isoflurane also interacts with E648, Y653, K656 and F659, while chloroform does it with F638, K639, L647 and L663 (Supplementary Material Table S2). The same site was experimentally identified and reported in TRPV1,¹⁹ highlighting that residue E600 is essential for TRPV1 activation by protons and Y653 by heat and anesthetics. Isoflurane sampled extensively the same region reported experimentally, while chloroform diffused fast through the pore site, presumably aided by its smaller size.

Site II' is equivalent to the binding site described in the literature for TRPV1 activators,²⁵ notably capsaicin. The pocket has dimensions of ~20 Å (E570-L662; C α distance) by 12 Å (T550-I668; C α distance), sufficient to accommodate the capsaicin molecule. In our simulations, this site is sampled by isoflurane and chloroform that reach the site via the lipophilic entry mechanism and a minor direct transition from the pore loop site I. The membrane-partitioned anesthetic diffuses into the vanilloid binding pocket (Site II'), which in this state of TRPV1 is open and solvent-exposed. In one case, entry into Site II' occurs through initial hydrophobic guidance across the protein-membrane interface with residues V318 and F522 of the S2-S3 transmembrane helices. In another case, diffusion into Site II' occurs via the opening at Site II mediated by L585 and I668, located at the interface between the membrane and the protein intrasubunit lumen. Both anesthetics make contacts with amino acid residues M547 and A665. In addition, isoflurane interacts with Y511, L515, T550, I569, L573 and L669

(Supplementary Material Figure S6.A) while chloroform interacts with a reduced number of amino acids: F591, I668 and L673 (Supplementary Material Figure S6.B). Alignment was made with the docked poses of capsaicin from previous work,²⁸ depicted in Fig. S5. In addition to structural overlap with capsaicin poses, an overlap of volatile general anesthetic contacts was observed with reported capsaicin contacts in TRPV1²⁸ for the down-conformation of capsaicin, Y511, L515, F543, M547, T550, A665, and L669, and for the up-conformation, Y511, L515, T550, F587, F591, I668, and L669. This site might constitute a potentiation or activation site of VGAs, akin to that of other TRPV1 agonists.

The side-pocket labelled site II located on the opposite side of the vanilloid binding pocket is flanked by the S4-S5 linker of one subunit, and the S6 P-loop of another subunit. Chloroform makes contacts with Y584, F580, M581, L664, T670, and I672 (Supplementary Material Table S2) while isoflurane sampled this site only transiently, moving into the adjoining site II' where it resided for up to 400 ns. Side-pocket site III was only sampled by chloroform and is a short-lived site, with contacts with Y565, R579, F580, V583, L674, M677 (Supplementary Material Table S2). This site is located in the space between S5 and S6 helices both from one subunit, and is a metastable site connecting Site II' of one subunit with Site II of another subunit (Figure 3). Finally, site IV is found in the space between helices S1, S2, S3 and S4. The interactions of the anesthetics in this site are with aromatic residues tyrosine and phenylalanine via π -stacking interactions; both isoflurane and chloroform make contacts with F488 and Y554. Isoflurane in addition interacts with Y441, Y495, F516, and N551 (Supplementary Material Figure Table S2) while chloroform does it with Y487, R491, F516, Y554 and Y555. The duration of these protein-ligand interactions is of hundreds of nanoseconds.

Complementing the MD simulations, a blind docking search on 500 representative snapshots of the TRPV1 transmembrane domain obtained from a holo-TRPV1 trajectory with capsaicin bound²⁸ revealed that site II' in the vanilloid binding pocket was the most populated (26.7% for isoflurane, 58% for chloroform), while the pore loop site I was the second hit (9% for isoflurane, 13% for chloroform), as detailed in Supplementary Material Table S3. This blind docking search was repeated on a TRPV1 trajectory without capsaicin bound, revealing that site II' remained most populated for isoflurane (18%) while the pore loop site I became the most populated for chloroform (44.1%). These results suggest that anesthetics could indeed act as secondary TRPV1 agonists in the absence of capsaicin.

It is known that binding of capsaicin induces activation in TRPV1 by stabilizing the open conduction state.²⁵ The reported²⁸ binding free-energy of capsaicin to TRPV1 is -10.6 ± 1.7 kcal mol⁻¹. It has been found that isoflurane does not bind in this site, and chloroform does not bind as strongly as capsaicin but it does so with a modest association found to be -2.0 ± 0.8 kcal mol⁻¹ (Supplementary Material Table S4). This suggests that the mechanism of action of anesthetics is different to the capsaicin mechanism of activation. It is known that volatile general anesthetics either activate or sensitize the channel to activation.²⁰ Sensitization seems more probable from the weak association of anesthetics in

Site II'. This can be partly explained due to their size, smaller than capsaicin, and their promiscuous binding poses.

Discussion and Conclusions

An understanding of the mechanisms by which general anesthetics modulate ion channels is essential to clarify the underlying behavior of ion channels and their role in reversible immobilization and amnesia. TRPV1 has distinct binding sites for its various agonists, and agonist binding is thus classed as allosteric. While capsaicin binds to the intracellular vanilloid binding side-pocket, protons bind to the extracellular outer-pore domain⁶⁸⁻⁶⁹ but both activate the channel.⁷⁰ Allosteric activation occurs by preferentially stabilizing the open-activated conduction state over a closed-inactivated state. The exact stoichiometry of TRPV1 agonist binding probed from patch clamp experiments revealed that while a single capsaicin site is required to achieve a fully conducting TRPV1 pore, proton agonists require binding to all four subunits to exert activating effects.²⁴ Currently, little is known about the sites at which drugs exert their influence. In addition, there is an ulterior motive for studying the interactions of volatile general anesthetics with TRPs which comes from the link between anesthesia and pain, and the observation that general anesthetics, through direct actions at TRP channels, increase postsurgical pain and inflammation.^{19, 71} In this study, we have focused on two general anesthetics chloroform and isoflurane; it has been reported that chloroform binds in dorsal root ganglion neurons to induce TRPV1 activation while clinically relevant concentrations of isoflurane were shown to sensitize TRPV1 to capsaicin and protons and reduce its threshold for heat activation.⁷¹ Imaging studies also found that chloroform and isoflurane act cooperatively with other TRPV1 agonists to induce a shift in the thermal activation of TRPV1 toward lower temperatures in the presence of mM concentrations of them.⁷¹ At present, the general view is that chloroform and isoflurane could active TRPV1 via similar mechanisms¹⁹ because they use overlapping sequence regions in the outer pore loop for activation, namely (i) residues required for proton and anesthesia activation (E600), and (ii) residues required for heat and anesthesia activation of TRPV1 (N628, N652, Y653).¹⁹ The mechanism of TRPV1 activation by anesthetics and the anesthetic interactions with TRPV1 remain unknown.

Translocation of anesthetics through the membrane from the bulk solution has been characterized by simulations with funnel-restrained metadynamics rendering a -3.4 ± 0.6 and -2.6 ± 0.8 kcal mol⁻¹ cost for isoflurane and chloroform respectively. Once inside the membrane, anesthetics diffuse to the protein. In this study, the anesthetics binding sites found in TRPV1 share common traits with four binding sites reported for isoflurane in nAChR and GLIC channels: at the pore, inter-subunit, intra-subunit, and annular sites.¹¹ Our computational work supports a model where anesthetics occupy multiple sites with a total of five sites identified, in agreement with experimental studies.^{19, 71} It has been proposed that chloroform and isoflurane could activate TRPV1 via similar mechanisms¹⁹ by using overlapping regions in the pore loop site I. This is in agreement with reported studies showing that hydrophilic-polar interfaces bind volatile anaesthetics.^{3-4, 18} Anesthetics access these sites from the bulk

solution through the cell membrane by diffusion. Anesthetic partitioning converged after 0.2 μ s with 95% of isoflurane and 90% of chloroform present in the membrane phase (Figure 2.B). The majority of bound anesthetic in TRPV1 entered through the lipophilic phase (100% of bound isoflurane, 92.5% chloroform), while a minority of events were observed for chloroform directly entering capsaicin site II' from the aqueous phase (Figure 2.A). Therefore, in TRPV1, the lipophilic mechanism was found to be predominant. Finally, the way chloroform and isoflurane sample the inner-core of the protein is different. Chloroform is smaller than isoflurane, and can access easily inner-protein regions that were banned for isoflurane (sites II, and III) at least on the timescale of these simulations.

Five binding sites for chloroform and three for isoflurane were characterized, the most long-lived of which are separated by up to 3 kcal mol⁻¹ from the other sites (Figure 4.A and C). Anesthetics do not induce new conformational states but rather only bind to pre-existing states. These binding sites correspond to site II' for chloroform and sites IV and II' for isoflurane. Site I, in the outer pore, shares protein-ligand contacts with the experimentally determined outer pore loop activation site of TRPV1. The binding site of capsaicin in TRPV1 was also identified as an anesthetic site (Site II'), although alchemical free-energy calculations suggest modest to no association when comparing the free-energy of binding for anesthetics with the reported value for capsaicin which suggest an alternative activation mechanism. The difference between site I and capsaicin site II' is the degree of hydrophobicity of each binding site. Site II' is characterized by a hydrophobic-non-polar interface (L515, T550, I569, L573, A665, and L669), while the pore site I is characterized by a hydrophilic-polar interface (E648, Y653, K656). The absence of significant structural rearrangements in the protein following anaesthetic binding is consistent with the weak interactions that are involved.

The data presented in this study provides information of the location of binding sites with moderate affinity as demonstrated by persistent occupancy. The absence of significant structural rearrangements in the protein following anaesthetic binding is consistent with the weak interactions that are involved. The atomistic information about where these drugs bind and the quantitative description of the interactions help rationalize how they modulate the function of this family of ion channels. Our simulations suggest that anaesthetics do not induce new conformational states but rather only bind to pre-existing states. As a consequence, they could exert their effects simply by shifting the equilibrium in favour of those conformations that contain anaesthetic-binding sites and in competition with TRPV1 agonists such as capsaicin. Uncovering chloroform and isoflurane modulatory sites will further our understanding of the TRPV1 molecular machinery and open the possibility of developing site-specific drugs that should lead to greater patient comfort.

Supporting Information. (1) Details of the MD simulation protocol; (2) RMSD profiles; (3) tables and distance profiles; (4) free-energy perturbation profiles and histograms, (5) free-energy corrections and metadynamics profiles. This material is available free of charge via the Internet at <http://pubs.acs.org>.

Author Information

Corresponding Authors: C.Domene@bath.ac.uk

Acknowledgements

The results of this research have been achieved using the DECI/PRACE resource Archer based in the UK at EPCC, Marconi based in CINECA in Italy, and SuperMUC based in Jülich in Germany with support from PRACE. C.J. thanks King's College London for a Graduate Teaching Assistant studentship.

Abbreviations

CNS, central nervous system; FEP, free energy perturbation; GABA, gamma-Aminobutyric acid; GLIC bacterial (*Gloeobacter*) ligand-gated ion channel; MD, molecular dynamics; nAChR nicotinic acetylcholine receptors; TRP, transient receptor potential; TRPV1 transient receptor potential vanilloid member 1; VGAs, volatile general anesthetics

References

1. Franks, N. P., General anaesthesia: from molecular targets to neuronal pathways of sleep and arousal. *Nature Reviews Neuroscience* **2008**, *9*, 370.
2. Hille, B., Local anesthetics: hydrophilic and hydrophobic pathways for the drug- receptor reaction. *The Journal of General Physiology* **1977**, *69* (4), 497-515.
3. Franks, N. P.; Jenkins, A.; Conti, E.; Lieb, W. R.; Brick, P., Structural Basis for the Inhibition of Firefly Luciferase by a General Anesthetic. *Biophysical Journal* **1998**, *75* (5), 2205-2211.
4. Bhattacharya, A. A.; Curry, S.; Franks, N. P., Binding of the general anesthetics propofol and halothane to human serum albumin. High resolution crystal structures. *J. Biol. Chem.* **2000**, *275* (49), 38731-8.
5. Vedula, L. S.; Brannigan, G.; Economou, N. J.; Xi, J.; Hall, M. A.; Liu, R.; Rossi, M. J.; Dailey, W. P.; Grasty, K. C.; Klein, M. L.; Eckenhoff, R. G.; Loll, P. J., A Unitary Anesthetic Binding Site at High Resolution. *Journal of Biological Chemistry* **2009**, *284* (36), 24176-24184.
6. Krasowski, M. D.; Harrison, N. L., General anaesthetic actions on ligand-gated ion channels. *Cellular and Molecular Life Sciences (CMLS)* **1999**, *55* (10), 1278-1303.
7. Yip, G. M. S.; Chen, Z.-W.; Edge, C. J.; Smith, E. H.; Dickinson, R.; Hohenester, E.; Townsend, R. R.; Fuchs, K.; Sieghart, W.; Evers, A. S.; Franks, N. P., A propofol binding site on mammalian GABAA receptors identified by photolabeling. *Nature Chemical Biology* **2013**, *9* (11), 715-720.
8. Eckenhoff, R. G., An inhalational anesthetic binding domain in the nicotinic acetylcholine receptor. *Proceedings of the National Academy of Sciences* **1996**, *93* (7), 2807-2810.
9. Nury, H.; Van Renterghem, C.; Weng, Y.; Tran, A.; Baaden, M.; Dufresne, V.; Changeux, J.-P.; Sonner, J. M.; Delarue, M.; Corringer, P.-J., X-ray structures of general anaesthetics bound to a pentameric ligand-gated ion channel. *Nature* **2011**, *469* (7330), 428-431.
10. Yuki, K.; Bu, W.; Xi, J.; Shimaoka, M.; Eckenhoff, R., Propofol shares the binding site with isoflurane and sevoflurane on leukocyte function-associated antigen-1. *Anesth. Analg.* **2013**, *117* (4), 803-11.
11. Brannigan, G.; LeBard, D. N.; Henin, J.; Eckenhoff, R. G.; Klein, M. L., Multiple binding sites for the general anesthetic isoflurane identified in the nicotinic acetylcholine receptor transmembrane domain. *Proceedings of the National Academy of Sciences* **2010**, *107* (32), 14122-14127.
12. Boiteux, C.; Vorobyov, I.; French, R. J.; French, C.; Yarov-Yarovoy, V.; Allen, T. W., Local anesthetic and antiepileptic drug access and binding to a bacterial voltage-gated sodium channel. *Proceedings of the National Academy of Sciences* **2014**, *111* (36), 13057-13062.
13. Vemparala, S.; Domene, C.; Klein, M. L., Interaction of Anesthetics with Open and Closed Conformations of a Potassium Channel Studied via Molecular Dynamics and Normal Mode Analysis. *Biophysical Journal* **2008**, *94* (11), 4260-4269.
14. Vemparala, S.; Saiz, L.; Eckenhoff, R. G.; Klein, M. L., Partitioning of Anesthetics into a Lipid Bilayer and their Interaction with Membrane-Bound Peptide Bundles. *Biophysical Journal* **2006**, *91* (8), 2815-2825.
15. Leffler, A.; Fischer, M. J.; Rehner, D.; Kienel, S.; Kistner, K.; Sauer, S. K.; Gavva, N. R.; Reeh, P. W.; Nau, C., The vanilloid receptor TRPV1 is activated and sensitized by local anesthetics in rodent sensory neurons. *The Journal of Clinical Investigation* **2008**, *118* (2), 763-776.
16. Marsakova, M. S. L.; Touska, M. S. F.; Krusek, R. N. D. P. J.; Vlachova, R. N. D. P. D. S. V., Pore Helix Domain Is Critical to Camphor Sensitivity of Transient Receptor Potential Vanilloid 1 Channel. *Anesthesiology* **2012**, *116* (4), 903-917.

17. Eckenhoff, R. G.; Johansson, J. S., Molecular interactions between inhaled anesthetics and proteins. *Pharmacological Reviews* **1997**, *49* (4), 343-367.
18. Liu, R.; Perez-Aguilar, J. M.; Liang, D.; Saven, J. G., Binding Site and Affinity Prediction of General Anesthetics to Protein Targets Using Docking. *Anesthesia & Analgesia* **2012**, *114* (5), 947-955.
19. Kimball, C.; Luo, J.; Yin, S.; Hu, H.; Dhaka, A., The Pore Loop Domain of TRPV1 Is Required for Its Activation by the Volatile Anesthetics Chloroform and Isoflurane. *Molecular Pharmacology* **2015**, *88* (1), 131-138.
20. Mutoh, T.; Tsubone, H.; Nishimura, R.; Sasaki, N., Effects of volatile anesthetics on vagal C-fiber activities and their reflexes in anesthetized dogs. *Respiration Physiology* **1998**, *112* (3), 253-264.
21. Venkatachalam, K.; Montell, C., TRP channels. *Annu. Rev. Biochem.* **2007**, *76*, 387-417.
22. Nilius, B.; Owsianik, G.; Voets, T.; Peters, J. A., Transient receptor potential cation channels in disease. *Physiol. Rev.* **2007**, *87* (1), 165-217.
23. Liao, M.; Cao, E.; Julius, D.; Cheng, Y., Structure of the TRPV1 ion channel determined by electron cryo-microscopy. *Nature* **2013**, *504* (7478), 107-112.
24. Hazan, A.; Kumar, R.; Matzner, H.; Priel, A., The pain receptor TRPV1 displays agonist-dependent activation stoichiometry. *Scientific Reports* **2015**, *5*, 12278.
25. Cao, E.; Liao, M.; Cheng, Y.; Julius, D., TRPV1 structures in distinct conformations reveal activation mechanisms. *Nature* **2013**, *504* (7478), 113-118.
26. Darré, L.; Furini, S.; Domene, C., Permeation and Dynamics of an Open-Activated TRPV1 Channel. *Journal of Molecular Biology* **2015**, *108* (2), 37a.
27. Jorgensen, C.; Furini, S.; Domene, C., Energetics of Ion Permeation in an Open-Activated TRPV1 Channel. *Biophys. J.* **2016**, *111* (6), 1214-1222.
28. Darré, L.; Domene, C., Binding of Capsaicin to the TRPV1 Ion Channel. *Molecular Pharmaceutics* **2015**.
29. Jo, S.; Kim, T.; Iyer, V. G.; Im, W., CHARMM-GUI: A web-based graphical user interface for CHARMM. *Journal of Computational Chemistry* **2008**, *29* (11), 1859-1865.
30. Buck, M.; Bouguet-Bonnet, S.; Pastor, R.; MacKerell Jr, A., Importance of the CMAP correction to the CHARMM22 protein force field: dynamics of hen lysozyme. *Biophysical Journal* **2006**, *90* (4), L36-L38.
31. Brooks, B.; Brooks, C.; MacKerell, A.; Nilsson, L.; Petrella, R.; Roux, B.; Won, Y.; Archontis, G.; Bartels, C.; Boresch, S., CHARMM: the biomolecular simulation program. *Journal of computational chemistry* **2009**, *30* (10), 1545-1614.
32. Klauda, J. B.; Venable, R. M.; Freites, J. A.; O'Connor, J. W.; Tobias, D. J.; Mondragon-Ramirez, C.; Vorobyov, I.; MacKerell, A. D.; Pastor, R. W., Update of the CHARMM All-Atom Additive Force Field for Lipids: Validation on Six Lipid Types. *The Journal of Physical Chemistry B* **2010**, *114* (23), 7830-7843.
33. Jorgensen, W. L.; Chandrasekhar, J.; Madura, J. D.; Impey, R. W.; Klein, M. L., Comparison of simple potential functions for simulating liquid water. *The Journal of chemical physics* **1983**, *79* (2), 926-935.
34. Hénin, J.; Brannigan, G.; Dailey, W. P.; Eckenhoff, R.; Klein, M. L., An Atomistic Model for Simulations of the General Anesthetic Isoflurane. *The Journal of Physical Chemistry B* **2010**, *114* (1), 604-612.
35. Yu, W.; He, X.; Vanommeslaeghe, K.; MacKerell, A. D., Extension of the CHARMM general force field to sulfonyl-containing compounds and its utility in biomolecular simulations. *Journal of Computational Chemistry* **2012**, *33* (31), 2451-2468.
36. Li, H.; Robertson, A. D.; Jensen, J. H., Very fast empirical prediction and rationalization of protein pKa values. *Proteins: Structure, Function, and Bioinformatics* **2005**, *61* (4), 704-721.
37. Phillips, J. C.; Braun, R.; Wang, W.; Gumbart, J.; Tajkhorshid, E.; Villa, E.; Chipot, C.; Skeel, R. D.; Kalé, L.; Schulten, K., Scalable molecular dynamics with NAMD. *Journal of Computational Chemistry* **2005**, *26* (16), 1781-1802.
38. Darden, T.; York, D.; Pedersen, L., Particle mesh Ewald: An N·log(N) method for Ewald sums in large systems. *The Journal of Chemical Physics* **1993**, *98* (12).
39. Verlet, L., Computer "Experiments" on Classical Fluids. I. Thermodynamical Properties of Lennard-Jones Molecules. *Physical Review* **1967**, *159* (1), 98-103.
40. Miyamoto, S.; Kollman, P. A., SETTLE: An analytical version of the SHAKE and RATTLE algorithm for rigid water models. *Journal of Computational Chemistry* **1992**, *13* (8), 952-962.
41. Tuckerman, M.; Berne, B. J.; Martyna, G. J., Reversible multiple time scale molecular dynamics. *The Journal of chemical physics* **1992**, *97* (3), 1990-2001.
42. Langevin, P., *On the theory of Brownian motion*. 1908.
43. Nosé, S., A unified formulation of the constant temperature molecular dynamics methods. *The Journal of Chemical Physics* **1984**, *81* (1), 511-519.
44. Nosé, S., A molecular dynamics method for simulations in the canonical ensemble. *Molecular physics* **1984**, *52* (2), 255-268.
45. Barducci, A.; Bussi, G.; Parrinello, M., Well-tempered metadynamics: a smoothly converging and tunable free-energy method. *Physical Review Letters* **2008**, *100* (2), 020603.

46. Limongelli, V.; Bonomi, M.; Parrinello, M., Funnel metadynamics as accurate binding free-energy method. *Proceedings of the National Academy of Sciences* **2013**, *110* (16), 6358-6363.
47. Bonomi, M.; Branduardi, D.; Bussi, G.; Camilloni, C.; Provasi, D.; Raiteri, P.; Donadio, D.; Marinelli, F.; Pietrucci, F.; Broglia, R. A.; Parrinello, M., PLUMED: A portable plugin for free-energy calculations with molecular dynamics. *Computer Physics Communications* **2009**, *180* (10), 1961-1972.
48. Gumbart, J. C.; Roux, B.; Chipot, C., Standard Binding Free Energies from Computer Simulations: What Is the Best Strategy? *Journal of Chemical Theory and Computation* **2012**, *9* (1), 794-802.
49. Gilson, M. K.; Given, J. A.; Bush, B. L.; McCammon, J. A., The statistical-thermodynamic basis for computation of binding affinities: a critical review. *Biophysical Journal* **1997**, *72* (3), 1047-1069.
50. Hermans, J.; Shankar, S., The free energy of xenon binding to myoglobin from molecular dynamics simulation. *Israel Journal of Chemistry* **1986**, *27* (2), 225-227.
51. Bennett, C. H., Efficient estimation of free energy differences from Monte Carlo data. *Journal of Computational Physics* **1976**, *22* (2), 245-268.
52. Shirts, M. R.; Chodera, J. D., Statistically optimal analysis of samples from multiple equilibrium states. *The Journal of chemical physics* **2008**, *129* (12), 124105.
53. Liu, P.; Dehez, F.; Cai, W.; Chipot, C., A Toolkit for the Analysis of Free-Energy Perturbation Calculations. *Journal of Chemical Theory and Computation* **2012**, *8* (8), 2606-2616.
54. Humphrey, W.; Dalke, A.; Schulten, K., VMD: Visual molecular dynamics. *Journal of Molecular Graphics* **1996**, *14* (1), 33-38.
55. Morris, G. M.; Huey, R.; Lindstrom, W.; Sanner, M. F.; Belew, R. K.; Goodsell, D. S.; Olson, A. J., AutoDock4 and AutoDockTools4: Automated docking with selective receptor flexibility. *Journal of Computational Chemistry* **2009**, *30* (16), 2785-2791.
56. Bernard, C., *Lec, ons sur les Anesth'esiques et sur L'Asphyxie*. Libraire J.- B. Balli`ere et fils: Paris, 1875; p 404.
57. Moore, B.; Roaf, H. E., On certain physical and chemical properties of solutions of chloroform and other anaesthetics: a contribution to the chemistry of anaesthesia. *Proc. R. Soc. Lond. B Biol. Sci.* **1905**, *77*, 86-102.
58. Moore, B.; Roaf, H. E., On certain physical and chemical properties of solutions of chloroform in water, saline, serum, and haemoglobin: a contribution to the chemistry of anaesthesia. *Proc. R. Soc. Lond. B Biol. Sci.* **1904**, *73*, 382-412.
59. Meyer, K. H., Contributions to the theory of narcosis. *Transactions of the Faraday Society* **1937**, *33* (0), 1062-1064.
60. Overton, E., *Studien über die Narkose: zugleich ein Beitrag zur allgemeinen Pharmakologie*. Gustav Fischer: 1901.
61. Smith, R. A.; Porter, E. G.; Miller, K. W., The solubility of anesthetic gases in lipid bilayers. *Biochim. Biophys. Act.* **1981**, *645* (2), 327-38.
62. Vorobyov, I.; Bennett, W. F. D.; Tieleman, D. P.; Allen, T. W.; Noskov, S., The Role of Atomic Polarization in the Thermodynamics of Chloroform Partitioning to Lipid Bilayers. *Journal of Chemical Theory and Computation* **2012**, *8* (2), 618-628.
63. Pohorille, A.; Wilson, M. A.; Chipot, C., Interaction of alcohols and anesthetics with the water-hexane interface: A molecular dynamics study. **1997**, *103*, 29-40.
64. Wieteska, J. R.; Welche, P. R. L.; Tu, K. M.; ElGamacy, M.; Csanyi, G.; Payne, M. C.; Chau, P. L., Isoflurane does not aggregate inside POPC bilayers at high pressure: Implications for pressure reversal of general anaesthesia. *Chemical Physics Letters* **2015**, *638*, 116-121.
65. Ursu, D.; Knopp, K.; Beattie, R. E.; Liu, B.; Sher, E., Pungency of TRPV1 agonists is directly correlated with kinetics of receptor activation and lipophilicity. *European Journal of Pharmacology* **2010**, *641* (2-3), 114-122.
66. Arcario, M. J.; Mayne, C. G.; Tajkhorshid, E., Atomistic Models of General Anesthetics for Use in in Silico Biological Studies. *The Journal of Physical Chemistry B* **2014**, *118* (42), 12075-12086.
67. Boiteux, C.; Vorobyov, I.; French, R. J.; French, C.; Yarov-Yarovoy, V.; Allen, T. W., Local anesthetic and antiepileptic drug access and binding to a bacterial voltage-gated sodium channel. *Proc. Natl. Acad. Sci.* **2014**, *111* (36), 13057-62.
68. Jordt, S.-E.; Julius, D., Molecular Basis for Species-Specific Sensitivity to "Hot" Chili Peppers. *Cell* **2002**, *108* (3), 421-430.
69. Jordt, S. E.; Tominaga, M.; Julius, D., Acid potentiation of the capsaicin receptor determined by a key extracellular site. *Proceedings of the National Academy of Sciences* **2000**, *97* (14), 8134-8139.
70. Nieto-Posadas, A.; Jara-Oseguera, A.; Rosenbaum, T., TRP Channel Gating Physiology. *Current Topics in Medicinal Chemistry* **2011**, *11* (17), 2131-2150.
71. Cornett, P. M.; Matta, J. A.; Ahern, G. P., General anesthetics sensitize the capsaicin receptor transient receptor potential V1. *Molecular Pharmacology* **2008**, *74* (5), 1261-1268.

Authors are required to submit a graphic entry for the Table of Contents (TOC) that, in conjunction with the manuscript title, should give the reader a representative idea of one of the following: A key structure, reaction, equation, concept, or theorem, etc., that is discussed in the manuscript. Consult the journal's Instructions for Authors for TOC graphic specifications.

